

Computational Investigation Of The Effect Of A Longitudinal Flat Blade Type Vortex Generator On The Turbulent Flow And The Thermal Flowfield Of A Rectangular Cross-Section Pipe

Trokas Nikolaos

Mechanical Engineering and
Aeronautics Dept.
University of Patras
Patras, Greece
nikostroks@gmail.com

Linardos Harris

Mechanical Engineering and
Aeronautics Dept.
University of Patras
Patras, Greece
calinard@upatras.gr

Margaris P. Dionissios

Mechanical Engineering and
Aeronautics Dept.
University of Patras
Patras, Greece
margaris@upatras.gr

Abstract—Vortex generators have emerged as a very promising method for heat transfer enhancement. In the present work, the effect of a vortex generator of longitudinal flat blade type on the flow and the thermal flowfield of a rectangular cross-section pipe is examined. The research became for six different aspect ratios of the pipe's cross-section and the width of the blade, and especially for pipe's aspect ratio (height / width) 3/2, 2/2, 1/2 and blade's / pipe's width equal to 0.1 and 0.05.

In the main part of the work, the rectangular pipe is designed with the blade inside at 30° angle. After that, the mesh is constructed and a mesh independence study is occurred. Then, the turbulence model $k-\epsilon$ Realizable is chosen and the appropriate boundary conditions are determined. Lastly, the simulation is running until the converge criterion for residuals of approximately $1e-05$ have reached.

The first simulations made for $Re=10000$ and found that model 2, with pipe's aspect ratio 3/2 and ratio of blade's / pipe's width 0.05, is the more efficient. In particular, it combines an adequate rise of 8% for Nusselt number and tolerable friction losses (only 5% increase).

Moreover, investigations made for various Reynolds number from 5000 to 20000. Found that the flat blade isn't suitable in high Re numbers, because doesn't affect significantly in heat transfer and causes considerable friction losses. Also, in low Re number, low aspect ratios models found to work better and, in medium Re number (≈ 10000) confirmed that model 2 is the best option above all.

Keywords—Turbulent flow; Vortex Generators; Heat Transfer Enhancement; CFD simulations;

I. INTRODUCTION

Ever-increasing energy demands and constraints on energy sources are enhancing the need for energy savings and more efficient ways of operating in many

industries. Many industrial applications such as refrigeration and air conditioning systems, aviation and automotive industry, petrochemical and general chemical industry etc., require efficient energy transfer and heating of the working fluid. Essentially, efficient heat transfer and reduction of pump work is sought to achieve high energy efficiencies and reduce the volume and cost of construction.

A promising method to achieve this purpose is the insertion into the flow of an obstacle, called Vortex Generator (VG) [1]. VGs were originally used to control separation on aircraft wings and in wind tunnels. In recent decades, however, it has been studied by many researchers to enhance its heat transfer performance. Found to enhance the mechanisms of heat transfer [2-5].

- generate secondary flows or turbulent flow by interrupting the surface
- mix the flow near the wall and in general, increasing the residence time of the fluid
- reduce the area of the thermal boundary layer
- enhance the turbulence intensity, by giving kinetic energy to the system

According to Modi and Rathod [6], there are many types of VGs such as delta wing, rectangular wing, delta winglet and rectangular winglet. They indicated that, when VG's trailing edge is attached to the surface, it is called wing and if VG's chord is attached to the surface, it is called winglet.

Fiebig [7], in 1998, and after plenty of studies, concluded that winglets cause higher heat transfer enhancement than wings.

However, afterwards, researchers studied the effect of rectangular wings in the flow and the heat transfer performance. Awais et al. [8] included in their review that wings induce longitudinal vortices that are found to be crucial on heat transfer enhancement. In other researches, Habchi and his colleagues, showed in two studies [9-10], that rows of rectangular wings enhance the mixing of the fluid inside a tube and that later on contributes to the heat transfer process. Moreover, Khoshvaght-Aliabadi et al. [11], studied

rows of wings in plate-fin and found that the rectangular type increases more the heat transfer performance.

That type of VG is investigated in this study, and its contribution to heat transfer enhancement is considered. The central idea is the insertion of a continuous rectangular wing, extending from the bottom of the duct to the top, without interruption.

II. GEOMETRY

The geometry domain is a pipe 500mm long, of rectangular cross-section. The investigation is made for 3 different aspect ratios of the pipe's cross-section and specifically for ratio of pipe's height / width equals to 3/2, 2/2 and 1/2.

The vortex generator is of longitudinal type and flat. It's placed 100mm from the inlet section with angle 30° with the horizontal plane. Two different widths are applied for each case to achieve ratios 0.1 and 0.05 in comparison with the pipe's width.

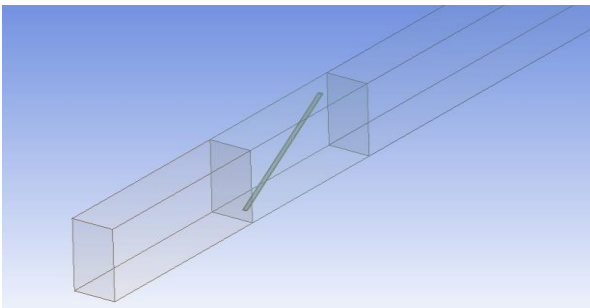


Figure 1: View of the system configuration

Model	1	2	3	4	5	6
Pipe's aspect ratio	3/2	3/2	2/2	2/2	1/2	1/2
Blade's / Pipe's width	0.1	0.05	0.1	0.05	0.1	0.05

Table 1: Characteristics aspect ratios of the models

III. MATHEMATICAL MODELLING

The three-dimensional incompressible steady flow and heat transfer numerical simulation is used. The continuity, momentum and energy equations that are used to solve the problem are as follows [12]:

A. Continuity equation

$$\frac{\partial(\rho u_i)}{\partial x_i} = 0 \quad (1)$$

B. Momentum equation

$$\frac{\partial(\rho \overline{u_i u_j})}{\partial x_j} = -\frac{\partial \bar{p}}{\partial x_i} + \frac{\partial}{\partial x_j} \left(\mu \left(\frac{\partial u_i}{\partial x_j} + \frac{\partial u_j}{\partial x_i} \right) \right) - \frac{\partial(\rho \overline{u_i u_j})}{\partial x_j} \quad (2)$$

C. Energy equation

$$\frac{\partial}{\partial x_i} \left(u_j (\rho e + p) \right) = \frac{\partial}{\partial x_j} \left(\kappa \frac{\partial T}{\partial x_j} \right) \quad (3)$$

IV. NUMERICAL INVESTIGATION

The present calculations were carried out by the ANSYS Fluent software, which discretizes and solves the governing equations with the finite volume method. Pressure based solver is used and Pressure-velocity coupling is achieved by the Coupled Algorithm for better convergence [12]. Convection terms discretized with second order upwind scheme and the diffusive terms with first order upwind scheme. The convergence criterion was set below 1e-04 for the continuity residual and below 1e-05 for all the other governing parameters.

The realizable k-ε model selected for the turbulent field because treats well swirling flows. The option enhanced wall treatment employed for more accurate resolution of the wall conditions. So, a y-plus (y⁺) value ≈5 is been applied. The turbulent kinetic energy, k, and its rate of dissipation, ε, are obtained from the following transport equations[12]:

$$\frac{\partial}{\partial x_j} (\rho k u_j) = \frac{\partial}{\partial x_j} \left[\left(\mu + \frac{\mu_t}{\sigma_k} \right) \frac{\partial k}{\partial x_j} \right] + G_b + G_k - \rho \varepsilon \quad (4)$$

$$\frac{\partial}{\partial t} (\rho \varepsilon) + \frac{\partial}{\partial x_j} (\rho k \varepsilon_j) = \frac{\partial}{\partial x_j} \left[\left(\mu + \frac{\mu_t}{\sigma_\varepsilon} \right) \frac{\partial \varepsilon}{\partial x_j} \right] + \rho C_{1\varepsilon} S \varepsilon - \rho C_{2\varepsilon} \frac{\varepsilon^2}{k + \sqrt{v \varepsilon}} + C_{1\varepsilon} \frac{\varepsilon}{k} C_{3\varepsilon} G_b \quad (5)$$

In these equations, G_k represents the generation of turbulence kinetic energy due to the mean velocity gradients, G_b is the generation of turbulence kinetic energy due to buoyancy, C₂, C_{1ε} and C_{3ε} are constants and σ_k and σ_ε are the turbulent Prandtl numbers for k and ε respectively.

μ_t is the turbulent viscosity and is computed as:

$$\mu_t = \rho C_\mu \frac{k^2}{\varepsilon} \quad (6)$$

where C_μ is a function of the mean strain and rotation rates, the angular velocity of the system rotation, and the turbulence fields.

V. PROPERTIES

For more accurate results, properties of the working fluid (air) didn't consider constant throughout

the process, but they are changing as a piecewise linear function between 273.15K and 650K.

VI. BOUNDARY CONDITIONS

In the inlet section the temperature is considered uniform, equal to 273.15K (0°C). The velocity is calculated from the Reynolds number expression. Turbulent intensity set for all the cases equal to 5%. In the wall, a constant wall temperature is considered equal to 650K. A pressure-outlet boundary condition applied at the outlet.

VII. IMPORTANT PARAMETERS

In order to neglect natural convection's effects, the Grashof number compared with the square of Reynolds number. The fraction was much less from 1, so convective heat transfer is dominant in this case.

For the evaluation of the results the following important parameters are used.

A. Friction factor

The friction factor is taken from the Pressure drop expression between two sections.

$$f = \frac{2\Delta P}{l \rho u_m^2} \quad (7)$$

where ΔP is the pressure drop through the pipe, l the length of the pipe, d the diameter, ρ the fluid's density and u_m the mean velocity.

B. Convective heat transfer coefficient

The convective heat transfer coefficient is taken from the Newton's cooling law and equals to:

$$h = \frac{q}{T_w - T_b} \quad (8)$$

T_w is the wall temperature,

T_b - bulk temperature is calculated as [9]:

$$T_b = \frac{\int u \rho c_p T dA}{\int u \rho c_p dA} \quad (9)$$

where u , ρ , c_p , T stand for the velocity, density, specific heat capacity with constant pressure, and the temperature of the fluid respectively.

And the overall heat flux q imported in an area is given by:

$$q = \frac{\dot{m} c_p (T_{out} - T_{in})}{A} \quad (10)$$

where c_p is the specific heat capacity at constant pressure, A the total heat transfer surface area of the pipe, T_{in} and T_{out} the inlet and outlet fluid temperature. \dot{m} the mass flow rate and is calculated as:

$$\dot{m} = \rho u A \quad (11)$$

and ρ is the density, u the inlet velocity and A the cross section of the pipe equals to $A = \frac{\pi d_h^2}{4}$.

D_h is the hydraulic diameter equals to:

$$d_h = \frac{4A}{\Pi} \quad (12)$$

with A the area and Π the perimeter of the cross-section.

C. Nusselt number

Nusselt number is defined from the heat transfer coefficient as:

$$Nu = \frac{h d_h}{k} \quad (13)$$

where h is the heat transfer coefficient and k the thermal conductivity of the fluid and d_h the hydraulic diameter of the pipe.

VIII. GRID INDEPENDENCE STUDY

In the areas far from VG a well-defined, fine, structured mesh was employed with hexahedral elements. In the wall, inflation technique was chosen to resolve efficiently the boundary layer. Ten layers were used and a value of $y^+ \approx 5$. Near to VG, multiple tetrahedral elements were selected because they adjust better in complex geometries.

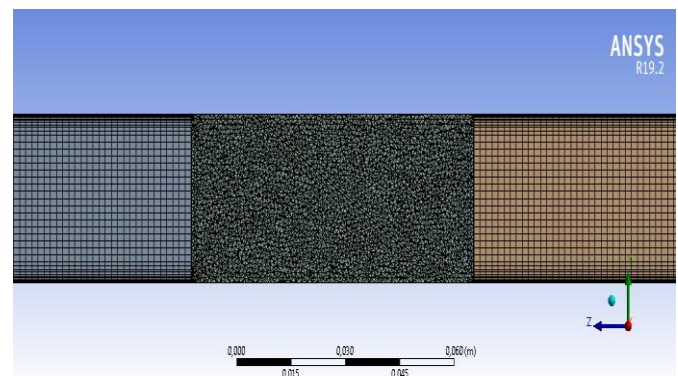


Figure 2: Meshing of the domain

Six different grids with various elements numbers were considered in order to minimize the meshing errors and enhance its sensitivity [4]. The study was made for model 1 and outlet bulk temperature used for the check. It can be seen from the diagram below that after 500000 elements the solution is normalized. Thus, considering accuracy and computation time the case with 520295 elements is selected for the computations. The error imported from this size of mesh is less than 0.02%.

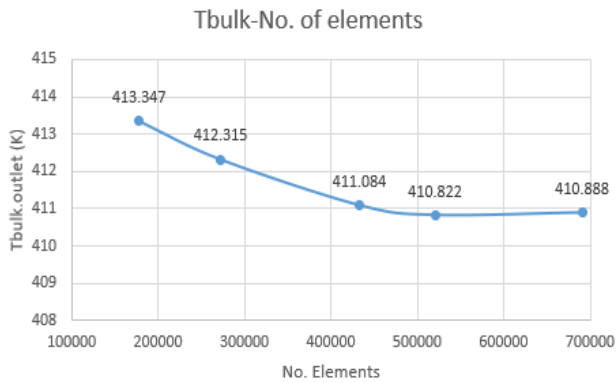


Figure 3: Grid independence study

To transport this study to the other cases, where pipe's dimensions are different (smaller), made a reduction 1mm^3 of fluid. In that way, found that for models 3 and 4 at least 346863.3 elements should use and for cases 5 and 6 at least 173431.7. In any case, the mesh concentration didn't surpass the original value of 520295 elements.

IX. RESULTS

In this section, the results of the simulations are discussed. Heat and flow characteristics of the different cases are examined and evaluated.

At first, Reynolds number equal to 10000 is used for the calculations.

In figures 4, 5 and 6 the bulk temperature across the tube is plotted. The expected shape of the bulk temperature for pipes with constant wall temperature is noted. Then, it is seen that an increase in the temperature values develops after VG interposes. A larger variation is observed in the models with larger blade's surface area, i.e., models 1, 3 and 5. The final temperature difference of these models with the corresponding plain tubes is about 10 degrees.

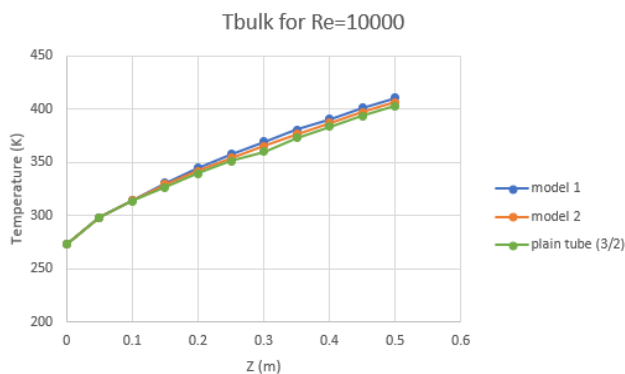


Figure 4: Tbulk for model 1,2 and the equivalent plain tube

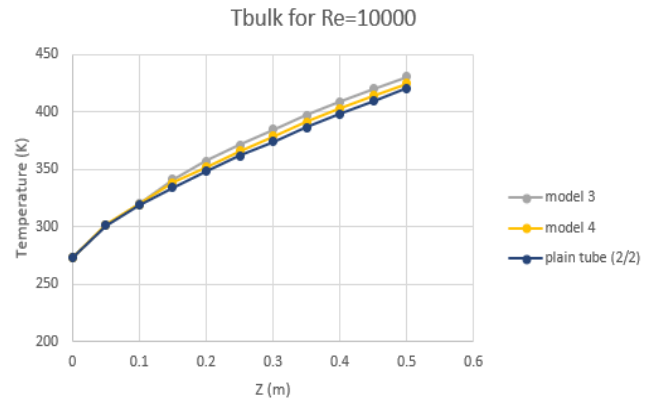


Figure 5: Tbulk for model 3,4 and the equivalent plain tube

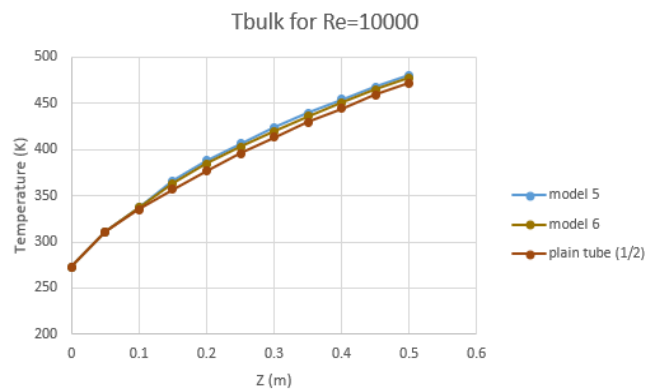


Figure 6: Tbulk for model 5,6 and the equivalent plain tube

After that, the response of heat transfer coefficient is investigated. The figures below show that VG agitates and heats up the fluid and then is brought to balance. Hence the increase of the coefficient in the interference blade region after 0.1m. Also, the wider VG appears to achieve higher h values than the thinner one, however this increase does not remain at later points of the pipeline.

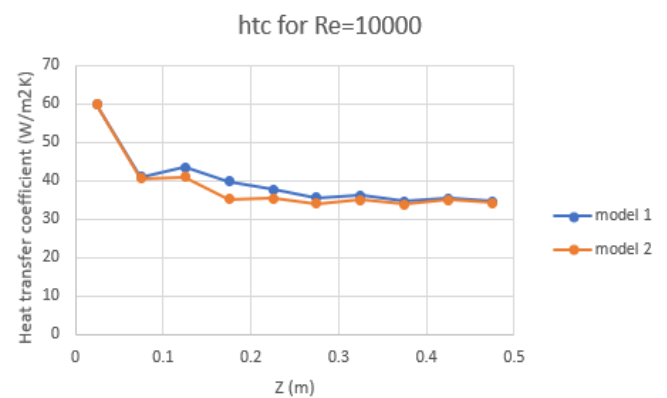


Figure 7: Heat Transfer coefficient for model 1 and 2

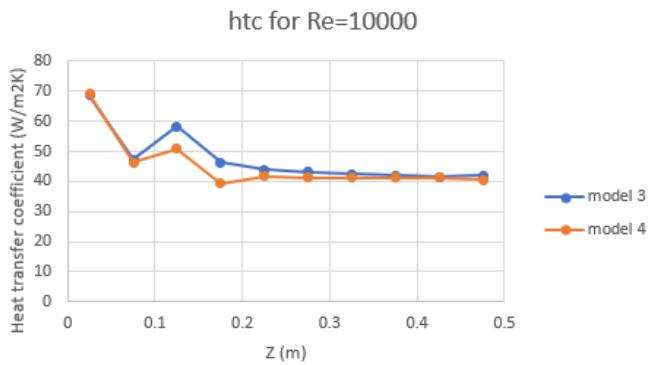


Figure 8: Heat Transfer coefficient for model 3 and 4

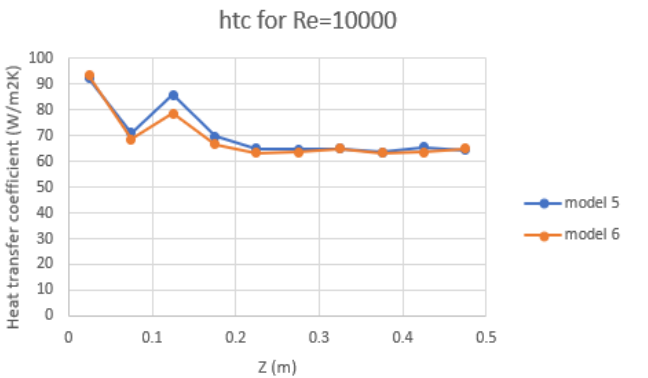


Figure 9: Heat Transfer coefficient for model 3 and 4

Similar to the bulk temperature diagrams, the values of the coefficient (as of temperature) are bigger in the shorter pipes. That's logical because the surface is smaller and that rises the fraction on the calculation of heat transfer coefficient. Also, in the case of the temperature, in smaller tubes there is less fluid to heat and as a result that happens easier. For those reasons, the dimensionless numbers of friction factor and Nusselt are of great importance. Because of this significance, the study of those parameters is generalized in various Re numbers from 5 to 20 thousand.

Figure 10 shows the change of friction factor for different Re values. It can be seen that the coefficient decreases with increasing Re number. Also, in models with high aspect ratio the coefficient is high and decreases as the pipeline height or/and the blade width decreases.

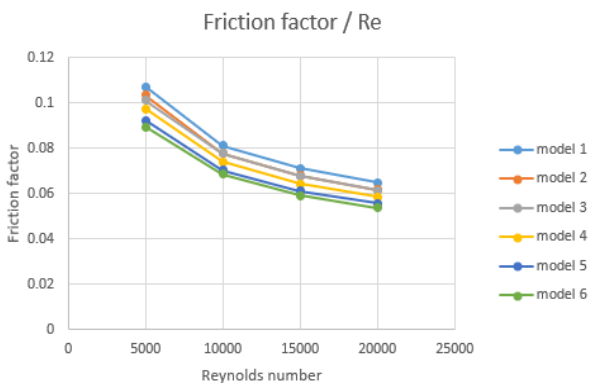


Figure 10: Friction factor for various Re numbers

In figure 11, the behavior of Nu number is presented. Initially, as expected, there is a clear increase in the Nusselt number with increasing Re number. Still a clear lead is observed for models 1 to 4 compared to models 5 and 6 with low aspect ratio. Their lead even increases for bigger Re numbers. Also, models with wider blade perform higher Nu numbers than those with the same pipe's aspect ratio and thinner blade.

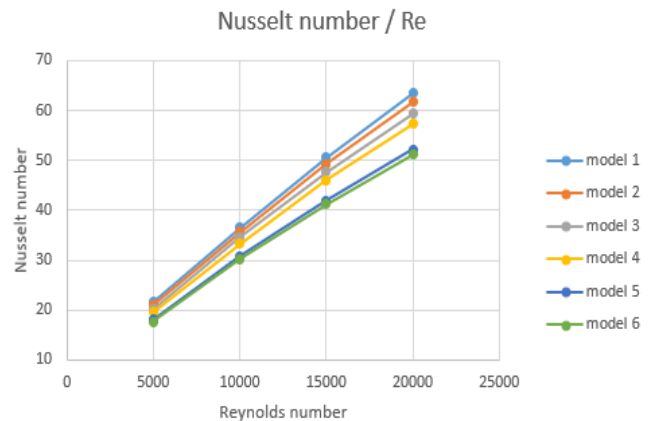


Figure 11: Nusselt number for various Re numbers

In this point, to access the true contribution of VG to the system performance, it is essential and meaningful to measure and analyze the changes that every model brings to its corresponding plain tube. It is not correct to keep the comparison only to the numerical values of the presented quantities, as each model has a different starting level. To be clear, the Nusselt number of a plain pipe with a 3/2 aspect ratio at 10000 Re is 43.9 while for a 2/2 aspect ratio's pipe 41.2. Thus, they cannot be compared directly, and the main investigation has to be extended to the percentage changes that the models bring to the empty pipes from which they originate (figure 12 and 13).

From figure 12 can be taken for the friction factor that, compared to the simple conductor, an increase in the value of about 5% is estimated for the thin VG models, while this figure doubles to about 10% with doubling the blade width. In models with a high aspect ratio, the factor is higher at every case.

Figure 13 shows that model 3 achieves a constant approximate 7% increase in Nusselt number for every case. This can be told also for model 5 which achieve increase 5-6%. At low Re numbers, those models work more effectively, as they achieve a satisfactory increase around 6%. Model 2 behaves extremely well in Re=10000, as it accomplishes an increase rate of 8% when in other Re numbers its value remains low. Furthermore, it is confirmed that model 4 and 6 have inadequate effect on heat transfer.

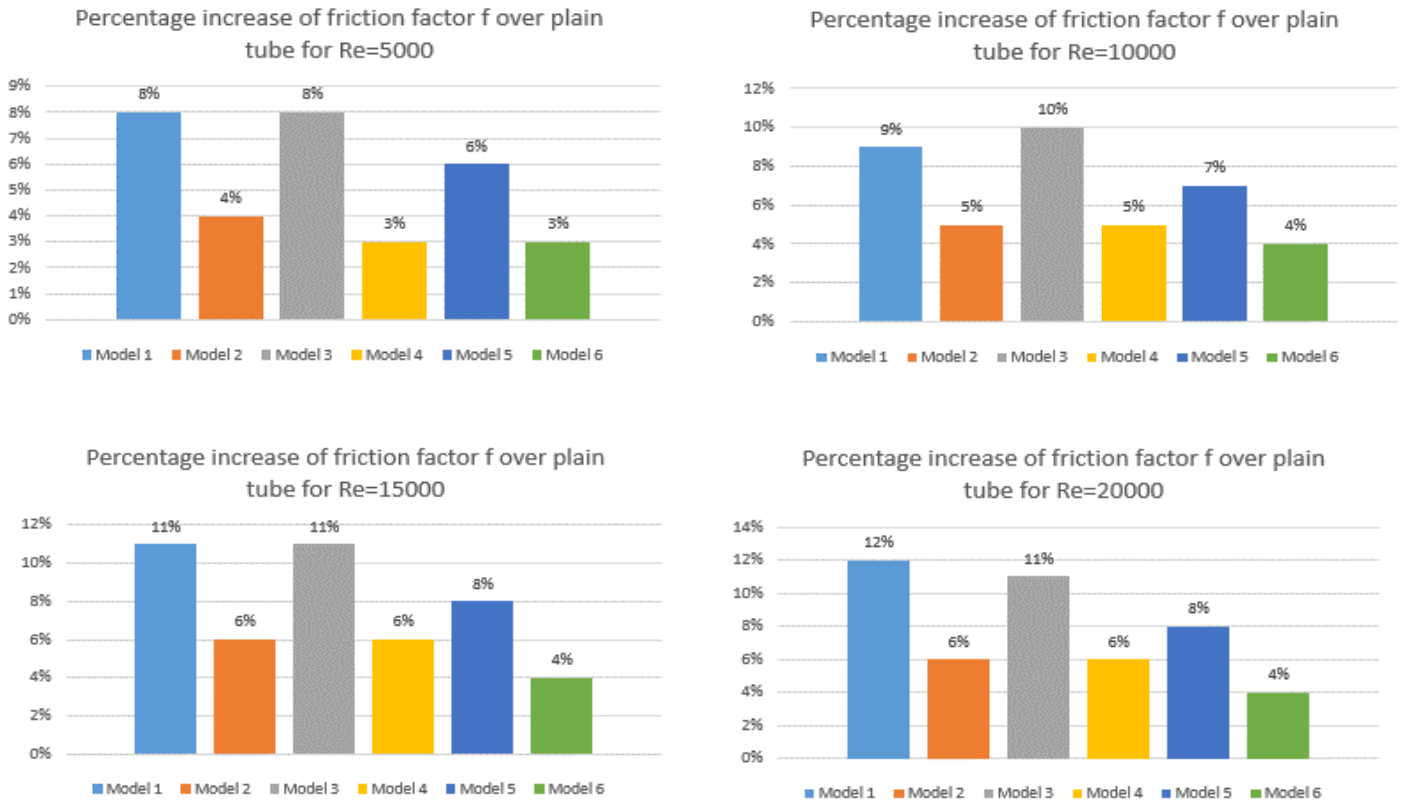


Figure 12: Percentage change on friction factor for each model over the relative plain tube

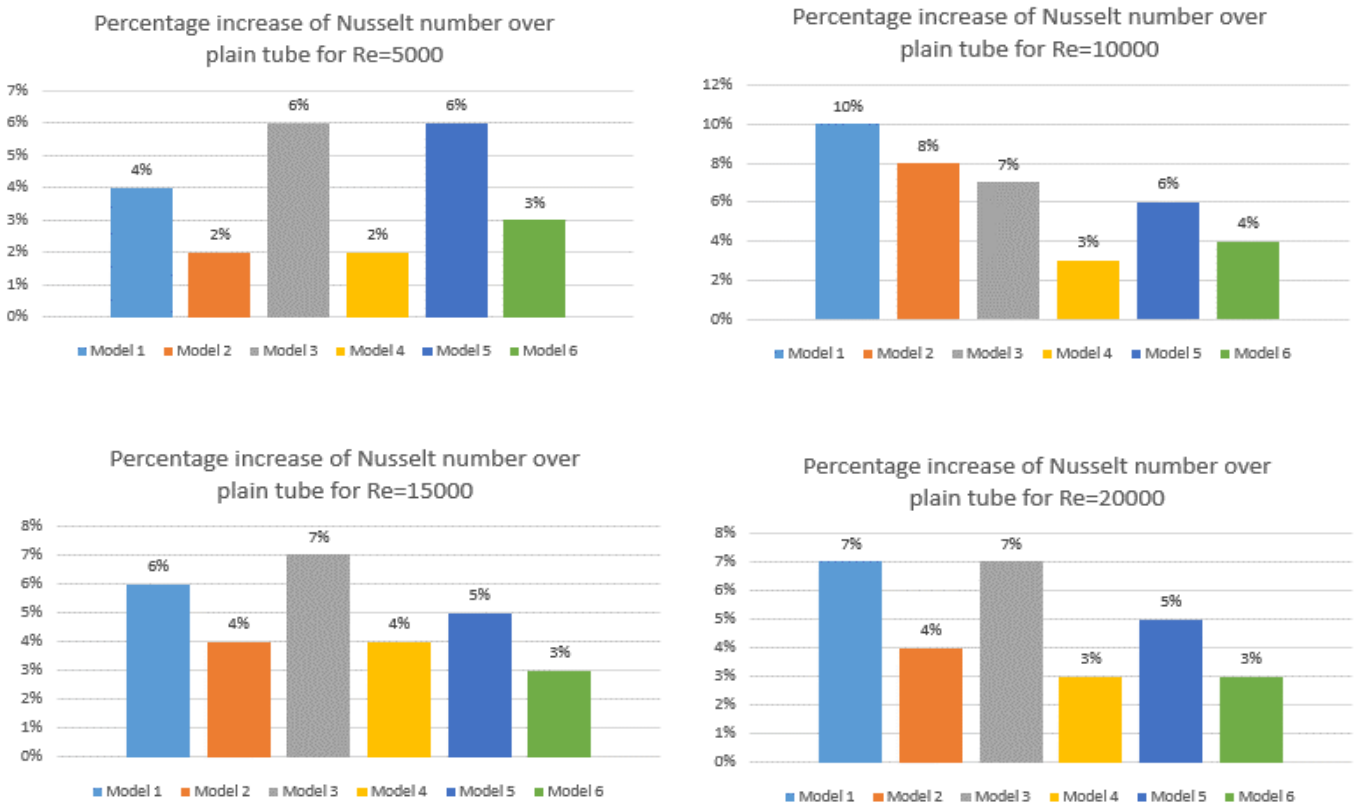


Figure 13: Percentage change on Nusselt number for each model over the relative plain tube

X. CONCLUSIONS

In general, as it is known, high Reynolds numbers benefits conductive heat transfer and reduce pressure losses.

After comparing analytically the percentage difference of friction factor and Nusselt number for the 6 models with the equivalent plain tubes, it is found that:

- At small numbers of Re, it seems that the low-height pipes (aspect ratio $\frac{1}{2}$) work more efficiently, since with this type of VG they manage to maintain similar rates of Nu increase to those of the friction factor, when in the other models the losses are much higher. Thus, model 5 is considered a good case, as it achieves a 6% increase in Nusselt number with proportional losses (6% increase in losses).
- At large Re numbers, the interference of this VG type does not contribute substantially, the rates of improvement of the Nu number are small and the losses are quite larger. Therefore, in this case, the blade mainly burdens the flow with additional friction losses.
- Finally, encouraging data are presented in pipes with large height and thin blade in the average Re numbers (≈ 10000). The simulation for model 2 at Re =10000 showed almost twice percentage increase in Nu number (8%) compared to the percentage increase in friction coefficient (less than 5%). Therefore, in this case, the effect of the VG is quite effective and contributes satisfactorily to the heat transfer enhancement of the system.

All in all, this rectangular type of VG can cause around 10% increase in Nu in some cases. Its main advantage is the relatively low and tolerable levels of friction losses in most of the cases.

REFERENCES

- [1] Akcayoglu A., (2011), Flow past confined delta-wing type vortex generators, *Experimental Thermal and Fluid Science*, Volume 35, Issue 1, pp. 112-120
- [2] Tusar M., Noman A., Islam M., Yarlagadda P., Salam B., (2019), CFD study oh heat transfer enhancement and fluid flow characteristics of turbulent flow through tube with twisted tape inserts, *Energy Procedia*, Volume 160, pp. 715-722

- [3] Awais M., Bhuiyan A.A., (2018), Heat transfer enhancement using different types of vortex generators (VGs): A review on experimental and numerical activities, *Thermal Science and Engineering Progress*, Volume 5, pp. 524-545
- [4] Wijayanta A.T., Istanto T., Keishi Kariya K., Miyara A., (2017), Heat transfer enhancement of internal flow by inserting punched delta winglet vortex generators with various attack angles, *Experimental Thermal and Fluid Science*, Volume 87, pp. 141-148
- [5] Wenbin Tu, Yun Wang, Yong Tang, (2016), A numerical study on thermal-hydraulic characteristics of turbulent flow through a circular tube fitted with pipe inserts, *Applied Thermal Engineering*, Volume 101, pp. 413–421
- [6] Ashish J. Modi, Manish K. Rathod, (2019), Comparative study of heat transfer enhancement and pressure drop for fin-and-circular tube compact heat exchangers with sinusoidal wavy and elliptical curved rectangular winglet vortex generator, *International Journal of Heat and Mass Transfer*, 141, pp. 310-326
- [7] Fiebig M., (1998), VORTICES, GENERATORS AND HEAT TRANSFER, *Chemical Engineering Research and Design*, Volume 76, Issue 2, pp 108-123
- [8] Awais M., Bhuiyan A.A., (2018), Heat transfer enhancement using different types of vortex generators (VGs): A review on experimental and numerical activities, *Thermal Science and Engineering Progress*, volume 5, pp. 524-545
- [9] Habchi C., Harion J-L., Russeil S., Bougeard D., Hachem F., Elmarakbi A., (2013), Chaotic mixing by longitudinal vorticity, *Chemical Engineering Science*, volume 104, pp. 439-450
- [10] Habchi C., Harion J-L., (2015), Enhanced mixing by optimized streamwise and angular positioning of longitudinal vorticity, *Applied Thermal Engineering*, volume 86, pp.269-280
- [11] Khoshvaght-Aliabadi M., Zangouei S., Hormozi F., (2015), Performance of a plate-fin heat exchanger with vortex-generator channels: 3D-CFD simulation and experimental validation, *International Journal of Thermal Sciences*, volume 88, pp 180-192

[12] ANSYS Inc, (2013), ANSYS Fluent Theory Guide, U.S.A.

[13] Huang X., Qingqing W., Zichen S., Yongguang Y., Haijun W., (2020), Heat transfer characteristics of supercritical water in horizontal double-pipe, Applied Thermal Engineering, volume 17